

***a-b* plane anisotropy of the superconducting gap in $\text{Bi}_2\text{Sr}_2\text{CaCu}_2\text{O}_{8+\delta}$**

C. Kendziora and A. Rosenberg

Naval Research Laboratory, Washington, D.C. 20375

(Received 7 August 1995)

We report *a-b* plane electronic Raman scattering (ERS) measurements of superconducting $\text{Bi}_2\text{Sr}_2\text{CaCu}_2\text{O}_{8+\delta}$ single crystals with T_c 's ranging from 90 K down to 65 K on both sides of the doping curve. At low temperatures, a peak associated with the opening of a superconducting energy gap $\Delta(\mathbf{k})$ forms in the electronic Raman continuum. Polarization selection rules yield ERS sensitivity to \mathbf{k} dependence and a clear anisotropy is observed. As the doping level is varied, anomalies in the observed continuum peak positions indicate that scattering in the B_{1g} symmetry is not a direct probe of $\Delta(\mathbf{k})$.

Of particular importance in cuprate superconductors are the dependencies of transition temperature (T_c) and order parameter symmetry, $\Delta(\mathbf{k})$, on doping level. Experiments sensitive to the \mathbf{k} dependence of Δ have shown considerable in-plane anisotropy in nearly optimally doped materials.¹⁻⁵ Low O_2 pressure anneals of $\text{YBa}_2\text{Cu}_3\text{O}_{7-\delta}$ have shown a considerable suppression of T_c , but the maximum T_c is reached for δ near zero and the overdoped region is largely inaccessible.⁶ Conversely, only the overdoped region has been accessed in Tl-based superconductors.⁷ Of the cuprates with T_c above 77 K, $\text{Bi}_2\text{Sr}_2\text{CaCu}_2\text{O}_{8+\delta}$ provides a unique opportunity to study both sides of the doping curve. Here, δ can be reversibly adjusted and T_c 's as low as 60 K can be obtained in both the underdoped and overdoped regimes.⁸

Through an appropriate choice of incident and scattered polarization vectors, Raman scattering from the electronic continuum is sensitive to different portions of the Fermi surface in \mathbf{k} space, and thus to anisotropy in $\Delta(\mathbf{k})$.^{9,10} In this Rapid Communication, we present a polarization dependent study of electronic Raman-scattering (ERS) measured above and below T_c for $\text{Bi}_2\text{Sr}_2\text{CaCu}_2\text{O}_{8+\delta}$ with variations in oxygen content. Our results provide evidence for three distinct doping regimes and for different physical phenomena in underdoped and heavily overdoped samples.

Single crystal samples of $\text{Bi}_2\text{Sr}_2\text{CaCu}_2\text{O}_{8+\delta}$ have been grown using a self-flux method described elsewhere.¹¹ The weak bonding between Bi-O layers allows for the (dis)intercalation of excess oxygen atoms (δ) during high-temperature anneals. The principle effects of oxygen intercalation are a decrease in the *c*-axis lattice parameter,¹² and an increased carrier concentration in the Cu-O planes.⁸

The individual crystals measured in this study are too small (1 mm \times 2 mm \times 10 μm) to precisely measure δ using direct techniques such as idiometric titration or thermogravimetric analysis. Instead, we rely on the more accurate measurements of T_c as a function of δ made on large polycrystalline $\text{Bi}_2\text{Sr}_2\text{CaCu}_2\text{O}_{8+\delta}$ samples available in the literature.¹³ After measuring T_c of our samples and knowing their annealing history, we then refer to the polycrystal data to assign an indexing value of δ for each sample. Table I gives T_c and the index δ for $\text{Bi}_2\text{Sr}_2\text{CaCu}_2\text{O}_{8+\delta}$ crystals measured using Raman scattering. These values of δ may be systematically shifted due to differences in cation stoichiometry but such errors in no way affect the implications of ERS data.

The 514 nm line of an Ar^+ laser was used for Raman excitation. Most of the data were collected using a line focus with incident power densities of 10–20 W/cm^2 . A comparison of the Stokes and anti-Stokes spectra indicates that the laser heated the sample locally by about 20 K at these power densities. Scattered light was collected in a near-backscattering geometry and a Dilor *XY* triple grating spectrometer was used to disperse the light onto a liquid nitrogen cooled charge-coupled-device array. The spectral resolution was set at 9 cm^{-1} . Stokes shifted spectra were measured between 30 and 1100 cm^{-1} .

Group theoretical consideration of Raman scattering in $\text{Bi}_2\text{Sr}_2\text{CaCu}_2\text{O}_{8+\delta}$ typically centers around its approximately tetragonal structure. For the $I4/mmm-D_{4h}^{17}$ space group, symmetry analysis^{14,15} predicts in-plane Raman active phonon modes of A_{1g} and B_{1g} symmetries, which can be selectively observed by appropriate choices of incident and scattered polarizations. In particular, the $z(XY)$ - z polarization measures scattering of B_{1g} symmetry, $z(XX)$ - z measures $A_{1g}+B_{1g}$, and $z(X'Y')$ - z measures B_{2g} . The experimental

TABLE I. A summary of the properties of $\text{Bi}_2\text{Sr}_2\text{CaCu}_2\text{O}_{8+\delta}$ single crystals analyzed with Raman scattering. Columns A_{1g} , B_{1g} , and B_{2g} denote the center frequency of the continuum peak for a given sample observed in that symmetry.

T_c		A_{1g}	B_{1g}	B_{2g}
(K)	δ	(cm^{-1})	(cm^{-1})	(cm^{-1})
68	0.24	300 \pm 10	310 \pm 20	335 \pm 20
70	0.23	315 \pm 10	390 \pm 20	
73	0.22	350 \pm 10	410 \pm 20	
79	0.21	370 \pm 10	445 \pm 20	415 \pm 20
85	0.19	385 \pm 15	490 \pm 20	
90	0.15	415 \pm 20	530 \pm 20	465 \pm 20
88	0.14	415 \pm 20	525 \pm 20	
86	0.13	385 \pm 20	550 \pm 20	475 \pm 20
84	0.11	...	540 \pm 20	
82	0.10	...	540 \pm 20	...
74	0.07	...	600 \pm 20	
68	0.06	...	610 \pm 20	
65	0.05	...	625 \pm 20	

fact that the B_{1g} phonon observed in XY at 285 cm^{-1} is not visible in XX indicates that this polarization is dominated by scattering with A_{1g} symmetry.

Because of polarization selection rules, different portions of the Fermi surface (FS) have different weights in the observed ERS. Variations in the effective mass tensor introduce \mathbf{k} dependence from the FS into the Raman vertex. To demonstrate how this arises we note that for the cuprate materials the skin depth ($\lambda \sim 1000\text{ \AA}$) is much longer than the coherence length ($\xi \sim 20\text{ \AA}$), and follow the calculations of Klein and Dierker¹⁶ and of Krantz and Cardona.¹⁷ In the limit $q(\propto \xi/\lambda) \rightarrow 0$ we arrive at an expression for the scattering efficiency from superconducting quasiparticle pairs:¹⁷

$$\frac{d^2S}{d\omega d\Omega} = r_0^2 \hbar N(E_F) \omega^{-1} m^2 \left[\langle \mu^{-2}\lambda \rangle - \frac{\langle \mu^{-1}\lambda \rangle^2}{\langle \lambda \rangle} \right]. \quad (1)$$

Here ω is the frequency, Ω the solid angle, r_0 the Thomson radius of the electron, $N(E_F)$ the density of states at the Fermi level, and m the mass of the electron. λ is the complex Tsuneto function¹⁸ evaluated on the FS. The imaginary part of λ is given by¹⁷

$$\lambda = \frac{4|\Delta(\mathbf{k})|^2}{\sqrt{\omega^2 - 4|\Delta(\mathbf{k})|^2}}. \quad (2)$$

μ is the Raman vertex which is given in the nonresonant limit by^{9,10}

$$\mu_{ij}(\mathbf{k}) = e^i \cdot \frac{1}{m^*} \cdot e^S = \frac{m}{\hbar^2} \sum_{i,j} e_i^i \frac{\partial^2 \varepsilon(\mathbf{k})}{\partial k_i \partial k_j} e_j^S. \quad (3)$$

Several aspects of the above formulas should be stressed. First, if the gap function $\Delta(\mathbf{k})$ were isotropic in \mathbf{k} , then the peak in the unscreened ERS spectrum [from Eq. (2)] would appear at an energy of 2Δ in all polarizations. Secondly, the second term in Eq. (1) takes Coulomb screening into account. It has been shown^{9,18} using symmetry arguments that this term is zero for both perpendicular polarizations pertaining to B_{1g} and B_{2g} symmetries. However, this term is non-negligible in the parallel polarization dominated by A_{1g} symmetry. The effect of such screening is to shift the peak down in energy to a value below 2Δ , suggesting that the peak measured in A_{1g} symmetry may not be simply related to the value of the gap.^{9,18} Third, the Raman vertex [Eq. (3)] weighs portions of the FS differently. In the present case, XY polarization (B_{1g} symmetry) has a $\cos(2\Phi)$ shape, with maxima along the k_x and k_y axes and a node at 45° .¹⁰ Conversely, the $X'Y'$ polarization (B_{2g}) has a $\cos(2\Phi + \pi/2)$ shape, similar to the XY but rotated by 45° .¹⁰ The XX polarization has a $\cos(4\Phi)$ dependence, indicating a dependence on portions of the FS both along the axes and along the diagonals, with the relative strengths of these maxima depending upon the details of the FS.^{19,20} Finally, Raman scattering is not sensitive to the sign of $\Delta(\mathbf{k})$, and so cannot distinguish between a d -wave gap and an anisotropic s -wave gap with a similar \mathbf{k} dependence.

Figures 1–3 show Raman spectra measured in the (Fig. 1) XX polarization (A_{1g} symmetry), (Fig. 2) XY polarization (B_{1g}), and (Fig. 3) $X'Y'$ polarization (B_{2g}) for $\text{Bi}_2\text{Sr}_2\text{CaCu}_2\text{O}_{8+\delta}$ single crystals with the values of δ

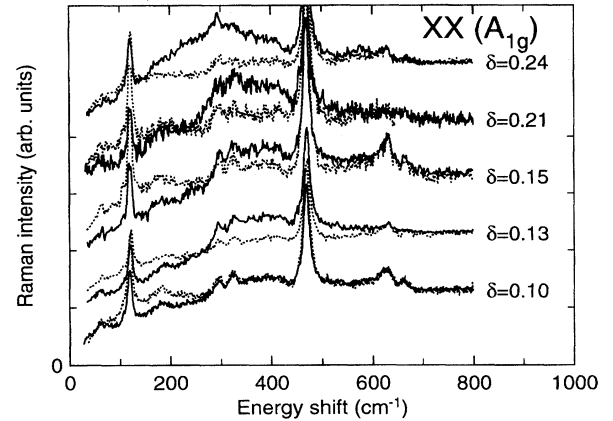


FIG. 1. Raman spectra observed at 30 K (solid lines) and 100 K (dashed lines) in the XX polarization (A_{1g} symmetry) for $\text{Bi}_2\text{Sr}_2\text{CaCu}_2\text{O}_{8+\delta}$. Tick marks along the vertical axis represent zero scattering for the offset spectra.

shown. For each polarization, spectra measured on the same sample at 100 K (dashed) and 30 K (solid) are scaled together at 1000 cm^{-1} , overlaid for comparison, and offset incrementally along the vertical axis. All of the spectra have been scaled by the thermal occupation Bose factor for the appropriate temperature. The curves have been cut off above 800 cm^{-1} in order to emphasize the low-frequency behavior. All of the data in Fig. 3 as well as the $\delta=0.10$ and 0.07 spectra in Fig. 2 have been smoothed in order to extract broad features.

In the XX polarization (Fig. 1) strong phonon modes are visible at 118 and 468 cm^{-1} , as are weaker ones at 295 , 315 , 630 , and 660 cm^{-1} . The electronic continua are relatively flat for the normal-state (100 K) spectra, independent of oxygen content. Below T_c , however, a broad peak forms in the electronic continuum and is accompanied by reduced scattering at the lowest shifts. This redistribution has been associated with the opening of a superconducting gap in these materials.^{2,9,10}

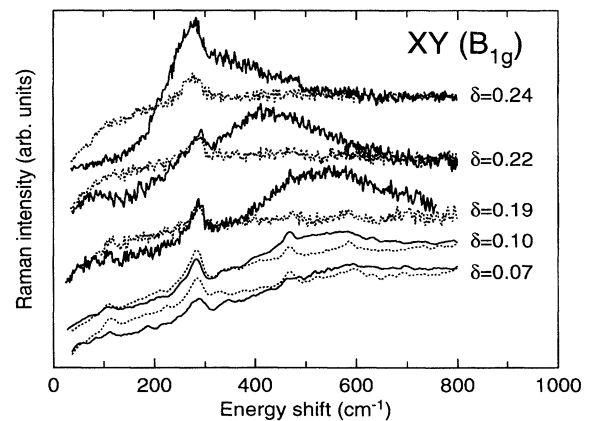


FIG. 2. Raman spectra observed at 30 K (solid lines) and 100 K (dashed lines) in the XY polarization (B_{1g} symmetry) for $\text{Bi}_2\text{Sr}_2\text{CaCu}_2\text{O}_{8+\delta}$.

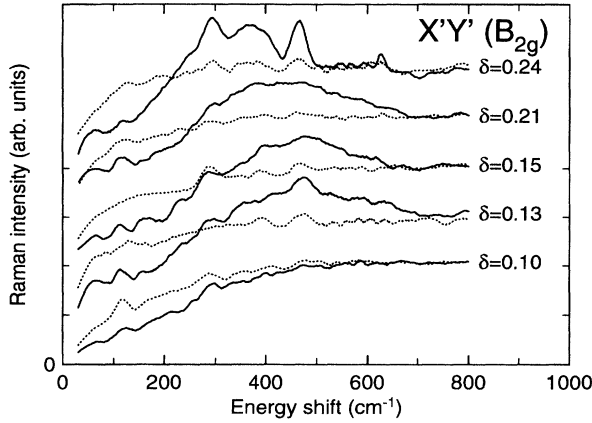


FIG. 3. Raman spectra observed at 30 K (solid lines) and 100 K (dashed lines) in the $X'Y'$ polarization (B_{2g} symmetry) for $\text{Bi}_2\text{Sr}_2\text{CaCu}_2\text{O}_{8+\delta}$. Tick marks along the vertical axis represent zero scattering for the offset spectra.

In underdoped samples with $T_c < 85$ K an A_{1g} peak does not form despite a significant loss of spectral weight at the lowest energies and temperatures. We consider several possible explanations for the disappearance of this continuum peak. The first is that the sample has lost thermal conductivity and is therefore warmed above T_c by the incident laser power. This is unlikely because the spectra are independent of power down to the lowest values used (2 W/cm^2) and because the loss of spectral weight near $100\text{--}200 \text{ cm}^{-1}$ indicates that the samples are indeed cold. A second possibility is that the laser is sampling a nonsuperconducting portion of the sample. This, too, is unlikely since we have never seen an A_{1g} continuum peak in any of ~ 15 underdoped samples, regardless of the area selected or the number of surface cleaves. Rather, we propose the more likely explanation that the samples simply have a low superfluid density²¹ and that the ERS is dominated by normal state carriers.²²

A peak forms in the B_{1g} continuum (Fig. 2) at low temperatures, but it is seen well into the underdoped regime. The broad peak seems to lose intensity and shift monotonically upward with decreasing δ , rather than scaling with sample T_c . In the $X'Y'$ polarization (Fig. 3) a B_{2g} continuum peak is clearly visible in the 30 K data for samples with $\delta \geq 0.13$, but not for the crystal with $\delta = 0.10$. As in A_{1g} and B_{1g} , this broad maximum shifts downward as the oxygen content is increased. In general, its position falls between those measured in A_{1g} and B_{1g} symmetries. Considering the \mathbf{k} dependence of these three symmetries from Eq. (3), the suppression of the A_{1g} peak energy below those of B_{1g} and B_{2g} requires a nonzero screening term in Eq. (1).

Figures 4(a) and 4(b) summarize the results of Figs. 1–3 and include samples omitted from these figures for clarity. Figure 4(a) plots the positions of the continuum peaks as functions of indexed oxygen content δ ; the values are listed in Table I. Figure 4(b) rescales this information after dividing each peak frequency by $k_B T_c$ for that crystal. Underdoped samples which did not show a continuum peak (denoted by “...” in Table I) have been omitted.

As a function of oxygen content δ , the ERS data appear to separate into three distinct regimes. In the slightly over-

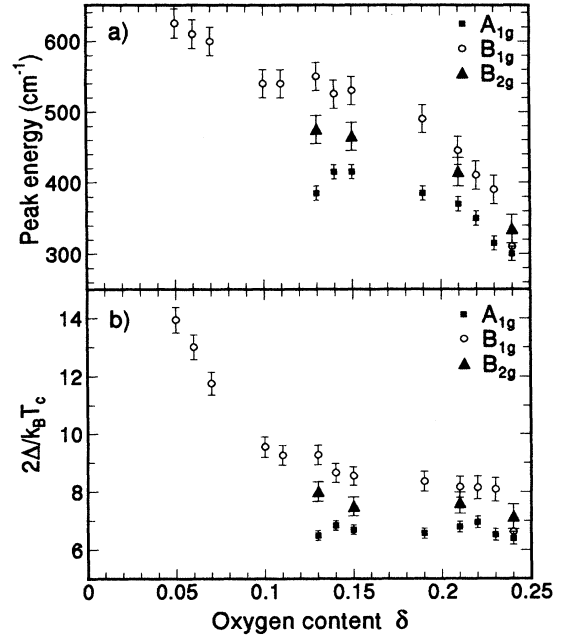


FIG. 4. (a) Absolute ERS continuum peak position vs δ . (b) Peak position divided by $k_B T_c$ of each sample vs δ .

doped regime, which is the only region where data are available in the literature,^{22–26} our spectra are similar to earlier results. Such measurements in this regime have been fit using a d -wave model⁹ as well as models based on a linear combination of isotropic and anisotropic order parameters ($s + d$).¹⁷ However, in the underdoped regime these models do not apply. Regardless of the reason for the lack of an A_{1g} peak in underdoped samples, the observation of a B_{1g} peak under identical conditions could be taken as evidence that the B_{1g} peak is not related to superconductivity. This argument is supported by the fact that the B_{1g} peak shifts monotonically upward in energy with a decrease in δ despite a decrease in T_c . Authors working with underdoped $\text{YBa}_2\text{Cu}_3\text{O}_{7-\delta}$ have made similar suggestions by noting that the B_{1g} peak is anomalously sensitive to doping level²⁷ and that it appears at temperatures above T_c .²⁸ It has been argued^{27,28} that in underdoped samples, the B_{1g} peak may be evidence for a pseudogap, either due to spin^{29,30} or phase²¹ fluctuations, which is observed only in this symmetry or only along the k_x or k_y portions of the FS to which it is sensitive.

Finally, in the heavily overdoped regime where $T_c < 75$ K, the continua in all three polarizations show the same peak value to within the experimental uncertainty. This result has been repeated for the B_{1g} and A_{1g} symmetries on several samples and suggests one of three possibilities. If both the A_{1g} and B_{1g} peaks are assumed to be direct measurements of the gap, then either (1) the gap is nearly isotropic or (2) “impurity” scattering associated with the extra oxygen atoms smears out the \mathbf{k} dependence of the ERS. Alternatively, (3) if the peak in B_{1g} is not directly related to superconductivity, then its overlap with the A_{1g} peak is coincidental. Consideration of the Coulomb screening favors case (3). If the A_{1g} peak energy is considered the screened average of the axial and diagonal gap values, then its overlap with the

B_{1g} peaks indicates that B_{1g} must now peak at a *lower* energy than B_{2g} . This is a reversal of the situation at lower doping levels. In any case, it is unfortunate that we cannot further overdope this material to investigate whether the B_{1g} peak appears at energies below A_{1g} and B_{2g} . However, measurements on very heavily overdoped $Tl_2Ba_2CuO_{6+\delta}$ ($T_c=30$ K) have shown that the B_{1g} continuum peak is pushed down to $3.5k_B T_c$ (from $8k_B T_c$ in an 85 K sample).³¹ The fact that this does not scale with T_c supports the inference that the B_{1g} peak is not a direct measurement of the superconducting gap energy.

In conclusion, polarization-dependent ERS measurements above and below T_c on $Bi_2Sr_2CaCu_2O_{8+\delta}$ demonstrate the existence of three distinct doping regimes. Although there are few changes in the normal-state spectra as a function of δ , underdoped samples show a continuum peak at low tem-

peratures only in B_{1g} symmetry. In the slightly overdoped regime, samples display continuum peaks in all symmetries, but at different energies, suggesting gap anisotropy. Finally, in heavily overdoped samples the continuum peaks in all symmetries appear at approximately the same energy. We argue that in the underdoped and heavily overdoped regimes, the B_{1g} continuum peak is not directly related to the opening of a superconducting gap. The physical interpretation of this B_{1g} peak will require further study.

We would like to acknowledge useful discussions with D. Branch, M. Cardona, X. K. Chen, T. P. Devereaux, L. Forro, R. Hackl, J. C. Irwin, M. V. Klein, M. C. Krantz, D. H. Leach, D. L. Peebles, W. E. Pickett, and T. J. Wieting. C.K. would like to acknowledge the financial support of the National Research Council.

-
- ¹Jeffrey Kane *et al.*, Phys. Rev. Lett. **72**, 128 (1994).
²M. Boekholt, M. Hoffmann, and G. Guntherodt, Physica C **175**, 127 (1991).
³Z. X. Shen *et al.*, Phys. Rev. Lett. **70**, 1553 (1993).
⁴R. J. Kelley *et al.*, Phys. Rev. Lett. **71**, 4051 (1993).
⁵H. Ding *et al.*, Phys. Rev. Lett. **74**, 2784 (1995).
⁶R. J. Cava *et al.*, Phys. Rev. Lett. **58**, 1676 (1987).
⁷Y. Shimakawa *et al.*, Phys. Rev. B **43**, 7875 (1991).
⁸C. Kendziora *et al.*, Phys. Rev. B **48**, 3531 (1993).
⁹T. P. Devereaux *et al.*, Phys. Rev. Lett. **72**, 396 (1994).
¹⁰X. K. Chen *et al.*, Phys. Rev. Lett. **73**, 3290 (1994).
¹¹C. Kendziora *et al.*, Phys. Rev. B **45**, 13 025 (1992).
¹²Yuichi Deshmaru *et al.*, Jpn. J. Appl. Phys. **30**, L1798 (1991).
¹³R. Sieburger *et al.*, Physica C **181**, 335 (1991).
¹⁴G. Burns *et al.*, Solid State Commun. **67**, 603 (1988).
¹⁵Ran Liu *et al.*, Phys. Rev. B **45**, 7392 (1992).
¹⁶M. V. Klein and S. B. Dierker, Phys. Rev. B **29**, 4976 (1984).
¹⁷M. C. Krantz and M. Cardona, J. Low Temp. Phys. **99**, 205 (1995).
¹⁸T. P. Devereaux *et al.*, Phys. Rev. Lett. **72**, 3291 (1994).
¹⁹T. P. Devereaux, A. Virosztek, and A. Zawadowski, Phys. Rev. B **51**, 505 (1995).
²⁰D. Branch and J. P. Carbotte, Phys. Rev. B **52**, 603 (1995).
²¹V. J. Emery and S. A. Kivelson, Nature (London) **374**, 434 (1995).
²²A. Yamanaka *et al.*, J. Phys. Chem. Solids **53**, 1627 (1992).
²³T. Staufer *et al.*, Phys. Rev. Lett. **68**, 1069 (1992).
²⁴A. Hoffmann *et al.*, J. Low Temp. Phys. **99**, 201 (1995).
²⁵D. H. Leach *et al.*, Solid State Commun. **88**, 457 (1993).
²⁶C. Kendziora and A. Rosenberg, Physica C **235-240**, 1121 (1994).
²⁷X. K. Chen *et al.*, Phys. Rev. B **48**, 10 530 (1993).
²⁸F. Slakey *et al.*, Phys. Rev. B **42**, 2643 (1990).
²⁹Mohit Randeria, Ji-Min Duan, and Lih-Yir Shieh, Phys. Rev. Lett. **62**, 981 (1989).
³⁰N. Nagaosa and P. A. Lee, Phys. Rev. B **45**, 966 (1992).
³¹G. Blumberg *et al.*, Physica C **235-240**, 1137 (1994).